Ruthenium Oxo Complexes of Macrocyclic Tertiary Amines. Synthesis, Electrochemistry, and Reactivities of Ruthenium Oxo Complexes of *meso*-2,3,7,11,12-Pentamethyl-3,7,11,17-tetra-azabicyclo[11.3.1]heptadeca-1(17),13,15-triene (L^1), and *X*-Ray Crystal Structure of *trans*-$[Ru^{IV}L^1(O)(NCO)]ClO_4$‡

Chi-Ming Che,* Wai-Tong Tang, Wai-On Lee, Wing-Tak Wong, and Ting-Fong Lai†
Department of Chemistry, University of Hong Kong, Pokfulam Road, Hong Kong

The new complexes *trans*-$[Ru^{III}L^1Cl_2]Cl$, *trans*-$[Ru^{IV}L^1(O)(NCO)]ClO_4$, and *trans*-$[Ru^{VI}L^1(O)_2][ClO_4]_2$ {L^1 = *meso*-2,3,7,11,12-pentamethyl-3,7,11,17-tetra-azabicyclo[11.3.1]heptadeca-1(17),13,15-triene} have been prepared. Their redox chemistry was studied in comparison with the related Ru–L^2–oxo system (L^2 = 1,4,8,11-tetramethyl-1,4,8,11-tetra-azacyclotetradecane). At pH 1.1, the E°_f of the *trans*-$[Ru^{VI}L^1(O)_2]^{2+}$/*trans*-$[Ru^{IV}L^1(O)(H_2O)]^{2+}$ couple occurs at 0.76 V *vs.* saturated calomel electrode. The complex cation *trans*-$[Ru^{IV}L^1(O)(NCO)]^+$ [space group $P\bar{1}$, a = 7.765(1), b = 10.714(1), c = 14.076(1) Å, α = 80.49(1), β = 86.03(1), γ = 88.11(1)°, Z = 2, and R = 0.034 for 3 629 observed Mo-K_α data] has been determined by *X*-ray crystallography. The Ru=O distance is 1.777(2) Å. The N–Me groups all lie on the same side of the macrocyclic ring. The complex *trans*-$[Ru^{VI}L^1(O)_2]^{2+}$ is capable of oxidizing alcohols, styrene, and toluene at room temperature.

There is a current interest in the design of ruthenium oxo complexes as selective oxidants for oxidation of organic substrates.[1-7] Recent work has shown that macrocyclic tertiary amines such as 1,4,8,11-tetramethyl-1,4,8,11-tetra-azacyclotetradecane L^2 enable the stabilization of high-valent ruthenyl (Ru=O) complexes in oxidation states IV, V, and VI.[2] However, for the Ru–L^2–oxo system, only *trans*-$[Ru^{V}L^2(O)Cl]^{2+}$ (electrochemically generated in solution) is capable of oxidizing alcohols to aldehydes at an appreciable rate at room temperature;[8] *trans*-$[Ru^{VI}L^2(O)_2]^{2+}$ and *trans*-$[Ru^{IV}L^2(O)X]^{n+}$ by contrast are relatively unreactive toward oxidation of olefins and alcohols.[1f] We are interested in the design of macrocyclic ruthenium oxo complexes which are active oxidants for organic substrates. The works of Meyer and others [1c,g,2,6,7] showed that high valent ruthenyl complexes of π-aromatic di-imines possess rich oxidation chemistry. Thus, we anticipated that incorporating a pyridine functional group into a macrocyclic tertiary amine ligand would enhance the oxidizing potential of the ruthenyl complex. The L^1 ligand [L^1 = *meso*-2,3,7,11,12-pentamethyl-3,7,11,17-tetra-azabicyclo [11.3.1]heptadeca-1(17),13,15-triene] has been synthesized recently,[9] and found to be resistant towards oxidation upon co-ordination to a metal ion. Moreover, the less basic but more nucleophilic nature of this ligand as compared with L^2 facilitates metal insertion. Herein, the synthesis, characterization, and reactivities of high valent ruthenium oxo complexes of L^1,[1f] found to be more reactive than their L^2 analogues, are described.

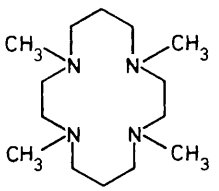

L^2

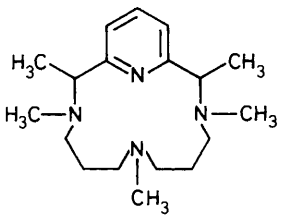

L^1

Experimental

Physical Measurements.—Elemental analyses of the newly prepared complexes were performed by Butterworth Laboratories Ltd. Infrared spectra were measured as Nujol mulls on a Perkin-Elmer 577 spectrophotometer (4 000—200 cm^{-1}), and u.v.–visible absorption spectra of freshly prepared solutions recorded with a Shimadzu UV240 spectrophotometer. Magnetic susceptibilities of solid samples were measured at room temperature by the Guoy method using mercury tetrathiocyanatocobaltate(II) as the calibrant. Cyclic voltammetry was performed using a Princeton Research (PAR) instruments model 175 Universal Programmer and model 173 Potentiostat-Galvanostat. The working electrodes were pyrolytic graphite and glassy carbon. A saturated calomel electrode (s.c.e.) was used as the reference electrode. When electrochemical studies were performed in a non-aqueous medium (acetonitrile), an Ag–$AgNO_3$ (0.1 mol dm^{-3} in CH_3CN) reference electrode was used and the ferrocenium–ferrocene couple was used as the internal standard. All solutions for electrochemical studies were deaerated using pre-purified argon gas. Controlled potential

† For correspondence on *X*-ray structure.
‡ *trans*-Isocyanato-oxo{*meso*-2,3,7,11,12-pentamethyl-3,7,11,17-tetra-azabicyclo[11.3.1]heptadeca-1(17),13,15-triene-$N^3N^7N^{11}N^{17}$}ruthenium(IV) perchlorate.

Supplementary data available: see Instructions for Authors, *J. Chem. Soc., Dalton Trans.*, 1989, Issue 1, pp. xvii–xx.

coulometry was performed using a PAR model 377A coulometric cell and a PAR model 179 digital coulometer. The working electrode was a glassy carbon cup (Atomergic Chemical V25-12).

Stoicheiometric oxidation of organic substrates by *trans*-$[Ru^{VI}L^1(O)_2][ClO_4]_2$ was performed by dissolving the ruthenium complex (20 mg) in acetonitrile (2 cm^3) containing the dissolved substrate. The reaction mixture was stirred with a magnetic stirrer and maintained at room temperature in a water bath. Controlled experiments in the absence of the ruthenium complex were also performed for each reaction. The products were analyzed by gas chromatography, ^1H n.m.r., mass spectrometry, and u.v.–visible spectroscopy. Gas chromatographic analyses were conducted using a Varian model 940 gas chromatograph with a flame ionization detector. The components were identified by comparing their retention times with that of an authentic sample and by gas chromatographic-mass spectral (g.c.–m.s.) analysis. Quantitation of individual gas chromatographic components was performed by the internal standard method employing a Shimadzu C-R3A electronic integrator.

X-Ray Crystal Structure of trans-$[Ru^{IV}L^1(O)(NCO)]ClO_4$.—*X*-Ray diffraction data were collected on an Enraf-Nonius CAD4 diffractometer with graphite monochromated Mo-K_α radiation (λ = 0.710 73 Å). The unit cell dimensions were obtained from a least-squares fit of 25 well centred reflections in the range $19 < 2\theta < 38°$. Three check reflections monitored every 2 h showed no significant variation in intensity. The intensity data were corrected for Lorentz and polarization effects but not for absorption.

The structure was solved by Patterson and Fourier methods and refined by full-matrix least squares. The perchlorate ion was disordered; two possible sites for the oxygen atoms were found each with an occupancy factor of 0.5. During the final cycles of the least-squares calculation the disordered oxygen atoms were refined isotropically while all other non-hydrogen atoms were refined anisotropically. The hydrogen atoms were generated geometrically (C–H 0.95 Å) with assigned isotropic thermal parameters and were allowed to ride on their attached carbon atoms. All calculations were carried out on a MICROVAX II computer using the Enraf-Nonius SDP programs.[10]

Crystal and structure determination data and the final agreement factors are given in Table 1, atomic co-ordinates of non-hydrogen atoms in Table 2, and selected bond distances and angles are given in Table 3.

Additional material available from the Cambridge Crystallographic Data Centre comprises H-atom co-ordinates, thermal parameters, and remaining bond lengths and angles.

Preparations.—trans-$[Ru^{III}L^1Cl_2]Y$ (Y = Cl *or* ClO_4). An ethanolic solution of the L^1 ligand (1.5 mmol in 200 cm^3) was added dropwise to a rigorously stirred ethanolic suspension of $K_2[RuCl_5(H_2O)]$ (0.5 g, 1.4 mmol) under reflux. The addition took 3 h for completion and the mixture was further refluxed for another 12 h. It was then filtered and the filtrate evaporated to dryness. The yellow solid obtained was recrystallized from hot HCl (2 mol dm^{-3}) to give crystals of *trans*-$[Ru^{III}L^1Cl_2]Cl$. The perchloric salt was obtained by metathesis reaction of the chloride salt with $NaClO_4$ (Found: C, 37.3; H, 5.5; Cl, 18.3; N, 9.7. Calc. for $[Ru^{III}L^1Cl_2]Cl$: C, 37.5; H, 5.6; Cl, 18.3; N, 9.7%). U.v.–visible spectrum (water): $\lambda_{max.}$ 385 nm ($\varepsilon_{max.}$ 3 170 $dm^3\ mol^{-1}\ cm^{-1}$) and 320 (2 060).

trans-$[Ru^{IV}(O)(NCO)]ClO_4$. The complex *trans*-$[Ru^{III}L^1Cl_2]Cl$ (0.3 g, 0.6 mmol) and silver(I) toluene-*p*-sulphonate (0.54 g, 2.0 mmol) in deionized water (25 cm^3) were heated to about 60 °C for 30 min. The resulting solution was filtered to remove the insoluble silver chloride. The filtrate was warmed to *ca.* 60 °C on a water bath. Sodium cyanate (0.1 g, 1.5 mmol) was added to the solution followed by H_2O_2 (50%, 1 cm^3). The solution was swirled until effervescence ceased. Additional NaNCO (0.1 g) was then added. The resulting brown solution was filtered to remove any insoluble material and solid $NaClO_4$ (0.5 g) was added to the filtrate. Upon cooling, golden brown needle-shaped crystals of *trans*-$[Ru^{IV}L^1(O)(NCO)]ClO_4$ slowly deposited. Yield ≈60% (Found: C, 38.3; H, 5.3; Cl, 16.7; N, 13.1. Calc. for $[RuL^1(O)(NCO)]ClO_4$: C, 38.1; H, 5.2; Cl, 6.6; N, 13.1%). U.v.–visible spectrum (CH_3CN): $\lambda_{max.}$ 302 nm ($\varepsilon_{max.}$ 5 170 $dm^3\ mol^{-1}\ cm^{-1}$) and 268 (4 130).

trans-$[Ru^{VI}L^1(O)_2][ClO_4]_2$. The complex *trans*-$[Ru^{III}L^1Cl_2]Cl$ (0.3 g, 0.6 mmol) and silver(I) toluene-*p*-sulphonate (0.54 g, 2.0 mmol) in deionized water (25 cm^3) were heated to *ca.* 60 °C for 30 min. The resulting solution was filtered to remove the insoluble silver chloride. H_2O_2 (50%, 3 cm^3) was slowly added to the filtrate while the solution was kept at 60 °C for 5 min. The solution was then cooled in an ice-bath. Upon addition of an excess of $NaClO_4$, yellow microcrystalline *trans*-$[Ru^{VI}L^1(O)_2][ClO_4]_2$ deposited gradually. This was filtered off and recrystallized from hot $HClO_4$ (0.1 mol dm^{-3}, 60 °C). Yield ≈60% (Found: C, 31.7; H, 4.5; Cl, 11.3; N, 9.3. Calc. for $[RuL^1(O)_2][ClO_4]_2$: C, 31.5; H, 4.6; Cl, 11.6; N, 9.2%). U.v.–visible spectrum (water): $\lambda_{max.}$ 400 nm ($\varepsilon_{max.}$ 720 $dm^3\ mol^{-1}\ cm^{-1}$), 320 (2 560), and 265 (7 900).

Table 1. Crystal data and summary of data collection and refinement

Formula	$C_{19}H_{32}ClN_5O_6$
M	563.02
Space group	$P\bar{1}$
a/Å	7.765(1)
b/Å	10.714(1)
c/Å	14.076(1)
α/°	80.49(1)
β/°	86.03(1)
γ/°	88.11(1)
U/Å^3	1 151.9
Z	2
$F(000)$	580
D_c/g cm^{-3}	1.623
D_m/g cm^{-3}	1.63
Crystal size/mm	0.32 × 0.29 × 0.19
μ(Mo-K_α)/cm^{-1}	8.3
Scan type, speed/° min^{-1}	ω—2θ; 1.6—5.5
Scan width/°	1.0 + 0.34 tanθ
T/K	292 ± 1
Collection range	$2\theta_{max.} = 50°$, $\pm h \pm kl$
Unique data	4 047
Observed data [$> 3\sigma(I)$], m	3 629 [$I > 3\sigma(I)$]
No. of parameters refined, p	285
$R = \Sigma\|\|F_o\| - \|F_c\|\|/\Sigma\|F_o\|$	0.034
$R' = [w(\|F_o\| - \|F_c\|)^2/\Sigma w\|F_o\|^2]^{\frac{1}{2}}$	0.055
$w = 4F_o^2/[\sigma^2(F_o^2) + (0.055\ F_o^2)^2]$	
$S = [\Sigma w(\|F_o\| - \|F_c\|)^2/(m - p)]^{\frac{1}{2}}$	1.67
Extrema in difference map (e Å^{-3})	+0.94 to −0.69

Results and Discussion

The synthesis of the ligand L^1 was reported previously.[9] We have found that this ligand readily forms complexes with Co^{II}, Ni^{II}, and Cu^{II}.[11] The Ru–L^1 complexes were prepared by a similar procedure as described for the Ru–L^2 analogues.[1f] The 'dropwise addition method' previously developed for the synthesis of *trans*-$[Ru^{III}L^3Cl_2]^+$ (L^3 = 1,4,8,11-tetra-azacyclotetradecane)[12] was adopted for the preparation of *trans*-$[Ru^{III}L^1Cl_2]Cl$. Removal of the chloro-groups of *trans*-$[Ru^{III}L^1Cl_2]Cl$ by Ag^I gave *trans*-$[Ru^{III}L^1(OH)(H_2O)]^{2+}$,

Table 2. Fractional atomic co-ordinates and thermal parameters for non-hydrogen atoms in $[RuL^1(O)(NCO)]ClO_4$ with estimated standard deviations (e.s.d.s) in parentheses

Atom	*x*	*y*	*z*	Atom	*x*	*y*	*z*
Ru	0.122 55(3)	0.208 90(2)	0.215 26(2)	C(12)	0.316 2(5)	0.262 5(4)	0.011 1(3)
O(1)	0.270 7(3)	0.174 3(2)	0.307 3(2)	C(13)	0.457 3(5)	0.109 3(4)	0.130 2(3)
O(2)	−0.201 6(4)	0.263 0(3)	−0.038 0(2)	C(14)	0.363 7(6)	−0.011 7(4)	0.124 9(3)
N(1)	−0.079 8(4)	0.188 1(3)	0.311 2(2)	C(15)	0.245 7(5)	−0.063 2(4)	0.212 7(3)
N(2)	0.087 0(4)	0.403 9(3)	0.236 5(2)	C(16)	−0.026 9(6)	−0.019 0(4)	0.137 0(3)
N(3)	0.349 7(4)	0.230 1(3)	0.114 7(2)	C(17)	−0.035 5(5)	−0.033 9(4)	0.309 1(3)
N(4)	0.076 8(4)	0.009 7(3)	0.216 9(2)	C(18)	0.066 4(7)	−0.084 1(4)	0.397 2(3)
N(5)	−0.045 3(4)	0.249 1(3)	0.101 6(2)	C(19)	−0.120 2(4)	0.257 1(3)	0.032 6(3)
C(1)	−0.150 7(5)	0.074 4(4)	0.333 3(3)	Cl	0.392 2(2)	0.307 4(1)	0.676 02(9)
C(2)	−0.310 6(6)	0.063 8(5)	0.385 4(3)	O(11)*	0.211(1)	0.319 5(8)	0.648 1(6)
C(3)	−0.384 1(5)	0.169 9(5)	0.416 2(3)	O(12)*	0.450(1)	0.200(1)	0.643 6(8)
C(4)	−0.300 0(5)	0.284 1(4)	0.400 0(3)	O(13)*	0.440(2)	0.427(1)	0.634(1)
C(5)	−0.143 0(5)	0.291 3(4)	0.345 9(3)	O(14)*	0.396(2)	0.300(1)	0.773 1(9)
C(6)	−0.018 4(5)	0.399 5(4)	0.333 1(3)	O(21)*	0.296(2)	0.300(1)	0.602 0(8)
C(7)	0.089 3(7)	0.383 1(4)	0.421 4(3)	O(22)*	0.371(1)	0.211(1)	0.758 4(8)
C(8)	−0.019 6(6)	0.484 4(4)	0.164 2(3)	O(23)*	0.398(1)	0.427 4(9)	0.706 0(7)
C(9)	0.259 3(6)	0.464 6(4)	0.236 4(3)	O(24)*	0.577(1)	0.305(1)	0.637 9(8)
C(10)	0.372 0(6)	0.459 0(4)	0.144 6(4)				
C(11)	0.461 6(5)	0.332 2(4)	0.139 3(3)				

* Atoms refined isotropically each with occupancy factor of 0.5.

Table 3. Selected bond distances (Å) and angles (°) for $[RuL^1(O)(NCO)]^+$

Ru–N(1)	1.994(3)	Ru–O(1)	1.777(2)
Ru–N(2)	2.165(4)	Ru–N(5)	2.115(3)
Ru–N(3)	2.178(3)	N(5)–C(19)	1.157(5)
Ru–N(4)	2.171(3)	C(19)–O(2)	1.206(5)
O(1)–Ru–N(1)	92.0(1)	N(2)–Ru–N(3)	98.9(1)
O(1)–Ru–N(2)	92.9(1)	N(2)–Ru–N(4)	161.7(1)
O(1)–Ru–N(3)	86.0(2)	N(2)–Ru–N(5)	88.0(1)
O(1)–Ru–N(4)	92.3(1)	N(3)–Ru–N(4)	99.0(1)
O(1)–Ru–N(5)	177.7(1)	N(3)–Ru–N(5)	91.8(1)
N(1)–Ru–N(2)	81.1(1)	N(4)–Ru–N(5)	87.5(1)
N(1)–Ru–N(3)	177.9(1)	Ru–N(5)–C(19)	168.8(4)
N(1)–Ru–N(4)	81.2(1)	N(5)–C(19)–O(2)	178.2(4)
N(1)–Ru–N(5)	90.2(1)		

which could be easily oxidized to *trans*-$[Ru^{VI}L^1(O)_2]^{2+}$ by H_2O_2 in water. Likewise, *trans*-$[Ru^{IV}L^1(O)(NCO)]ClO_4$ was prepared by digesting *trans*-$[Ru^{III}L^1Cl_2]^+$ with silver(I) toluene-*p*-sulphonate in water for 30 min followed by H_2O_2 oxidation in the presence of NaNCO. The salt *trans*-$[Ru^{V}L^1(O)_2]ClO_4$ has been generated electrochemically by reduction of *trans*-$[Ru^{VI}L^1(O)_2]^{2+}$ in acetonitrile at −0.2 V. No attempt was made to isolate this complex since it has been found to be very hygroscopic.

The newly prepared ruthenium complexes are air-stable solids. The dioxoruthenium(VI) complex is diamagnetic as expected for a d^2-dioxometal complex. The measured room-temperature $\mu_{eff.}$ for Ru^{III} is 1.88 corresponding to the spin-only value of one unpaired electron. The structure of *trans*-$[Ru^{IV}L^1(O)(NCO)]ClO_4$ which has been established by *X*-ray crystallography is described in a later section.

The u.v.–visible spectrum of *trans*-$[Ru^{III}L^1Cl_2]^+$ shows only one intense band at 380 nm assignable to a $p_\pi(Cl) \longrightarrow d_\pi(Ru)$ charge-transfer transition. Since only one ligand-to-metal charge transfer (l.m.c.t.) transition is observed, the metal complex is likely in the trans configuration.[13] The complexes *trans*-$[Ru^{VI}L^1(O)_2]^{2+}$ and *trans*-$[Ru^{V}L^1(O)_2]^+$ show vibronic structured $d_{xy} \longrightarrow d_\pi^*$ ($d_\pi^* = d_{xz}, d_{yz}$) transitions at 385 and 433 nm respectively (Figure 1), which is the characteristic u.v.–visible spectral feature of *trans*-dioxoruthenium-(VI) and -(V) complexes of macrocyclic amines.[1f] The i.r. spectrum of *trans*-$[Ru^{VI}L^1(O)_2]^{2+}$ shows one intense ν_{asym}(Ru=O) stretch at 860 cm^{-1}. For *trans*-$[Ru^{IV}L^1(O)(NCO)]^+$, the (Ru=O) stretch occurs at a lower frequency of ≈790 cm^{-1}, in accordance with the bonding structure, that the $Ru^{IV}=O$ system should have a weaker metal-oxo bond than Ru^{VI} [Ru^{IV}, $(d_{xy})^2(d_{xz})^1(d_{yz})^1$; Ru^{VI}, $(d_{xy})^2$].[1f]

Structural Description of trans-$[Ru^{IV}L^1(O)(NCO)]ClO_4$.—Figure 2 shows the ORTEP drawing with atomic numbering scheme for the *trans*-$[Ru^{IV}L^1(O)(NCO)]^+$ cation. The co-ordination geometry about the Ru atom is distorted octahedral with the oxo and NCO groups *trans* to each other and the metal atom in the mean plane of the four equatorial N atoms. The angle N(5)–Ru–O(1) unit is slightly bent [177.7(1)°]; *cf.* *trans*-$[Ru^{IV}L^2(O)X]^{n+}$ (X = NCO, NCO–Ru–O 178.2; X = N_3, N_3–Ru–O 177.6; X = Cl, Cl–Ru–O 177.2°).[1f] The distortion of the O–Ru–NCO axis is possibly a consequence of the non-bonded repulsive interactions of the N–Me groups with the axial ligands.

The L^1 ligand in the ruthenium complex is essentially planar. All the N–Me groups are directed to the same side; towards the NCO and *anti* to the two C–Me groups. This is in contrast to the complexes $[CoL^1Cl]ClO_4$,[9] $[NiL^1Cl]ClO_4$,[11] and $[NiL^1][ClO_4]_2 \cdot 2H_2O$ [11] in which the N–Me groups are oriented in a 'two up one down' manner. The five- and six-membered chelated rings of the L^1 ligand have envelope and chair conformations respectively.

The Ru–N(NCO) distance of 2.115(3) Å is comparable to the analogous value of 2.116 Å found in *trans*-$[Ru^{IV}L^2(O)(NCO)]ClO_4$.[1f] The Ru–N (tertiary amine) distances, which fall within the range 2.16—2.18 Å, are comparable to those found in other ruthenium macrocyclic tertiary amine complexes.[1f] The Ru–N(pyridine) distance of 1.994(3) Å is shorter, as expected for the sp^2 hybridized N atom. An important structural feature of *trans*-$[Ru^{IV}L^1(O)(NCO)]^+$ is the Ru=O distance of 1.777(2) Å, which is longer than that found in *trans*-$[Ru^{IV}L^2(O)X]^{n+}$ [*d*(Ru=O) 1.765 Å).[1f] Previous work [1f] showed the Ru=O distances of the *trans*-$[Ru^{IV}L^2(O)X]^{n+}$ system are insensitive to the nature of the *trans*-ligand X. Thus the elongation of the Ru=O bond from *trans*-$[Ru^{IV}L^2(O)(NCO)]^+$ to *trans*-$[Ru^{IV}L^1(O)(NCO)]^+$ is likely due to the pyridine functional group of L^1, which weakens the metal–oxo bond through coulombic repulsive interactions of the pyridine p_π electrons with the p_π–d_π electrons of the Ru=O

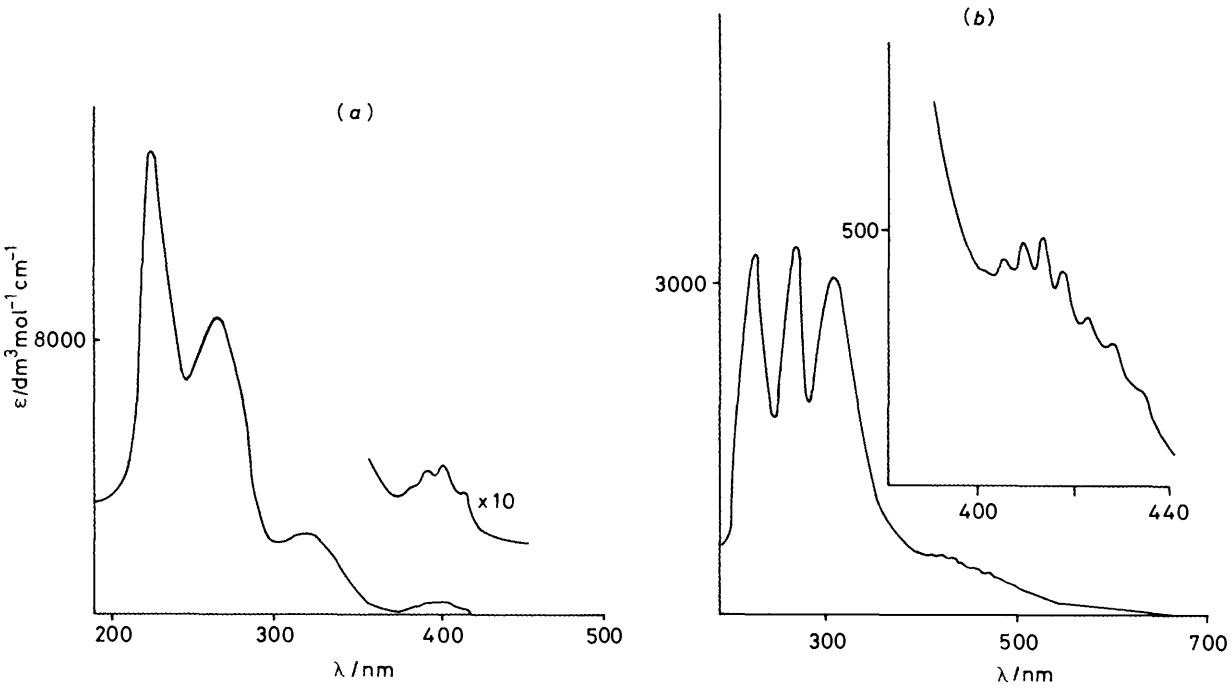

Figure 1. U.v.–visible absorption spectra of *trans*-$[Ru^{VI}L^1(O)_2]^{2+}$ (*a*) and *trans*-$[Ru^{V}L^1(O)_2]^{+}$ (*b*) in acetonitrile showing vibronic structured $d_{xy} \longrightarrow d_{\pi^*}$ transitions

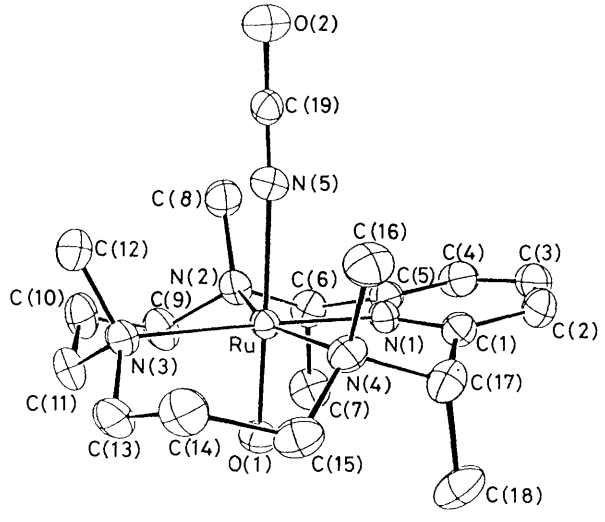

Figure 2. ORTEP drawing and atomic numbering scheme of the [Ru-L^1(O)(NCO)]$^+$ cation (35% probability ellipsoids)

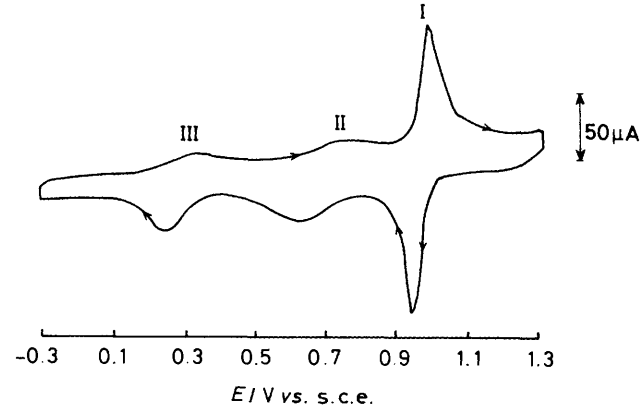

Figure 3. Cyclic voltammogram of *trans*-$[Ru^{VI}L^1(O)_2]^{2+}$ in 0.1 mol dm^{-3} CF_3SO_3H with pyrolytic graphite (edge plane) as the working electrode; scan rate, 50 mV s^{-1}

bond. A more pronounced effect is observed in *trans*-$[Ru^{IV}(py)_4(O)Cl]^+$ (py = pyridine), with an observed Ru=O distance of 1.862 Å.[14]

Electrochemistry in Aqueous Solution.—The electrochemistry of *trans*-$[Ru^{VI}L^1(O)_2]^{2+}$ (**1**) is similar to its L^2 analogue. The cyclic voltammogram of (**1**) (Figure 3) in 0.1 mol dm^{-3} CF_3SO_3H shows three reversible/quasi-reversible couples I, II, and III at potentials of 0.76, 0.52, and 0.07 *vs.* s.c.e. respectively, corresponding to the electrode reactions (1)—(3).

$$trans\text{-}[Ru^{VI}L^1(O)_2]^{2+} + 2H^+ + 2e^- \longrightarrow trans\text{-}[Ru^{IV}L^1(O)(H_2O)]^{2+} \quad (1)$$

$$trans\text{-}[Ru^{IV}L^1(O)(H_2O)]^{2+} + H^+ + e^- \longrightarrow trans\text{-}[Ru^{III}L^1(OH)(H_2O)]^{2+} \quad (2)$$

$$trans\text{-}[Ru^{III}L^1(OH)(H_2O)]^{2+} + H^+ + e^- \longrightarrow trans\text{-}[Ru^{II}L^1(H_2O)_2]^{2+} \quad (3)$$

Controlled-potential reduction of (**1**) in 0.1 mol dm^{-3} CF_3SO_3H with potentials held at 0.63, 0.25, and −0.1 V *vs.* s.c.e. established $n = 2$ for couple I and $n = 1$ for couples II and III. When the pH of the medium is raised the redox couples shift cathodically. The Pourbaix diagram of the formal potentials *versus* the pH of the medium over the range pH 1—12 is shown in Figure 4, and the results are summarized in Table 4.

The formal potentials of the electrode reaction are governed by the Nernst equation (4) where n = number of electrons and

$$E_f = E_f^\circ + (2.303RT/nF)\log[H^+]^m = E_f^\circ - (0.059m/n)\text{pH} \quad (4)$$

m = number of protons involved in the half-cell reduction process.

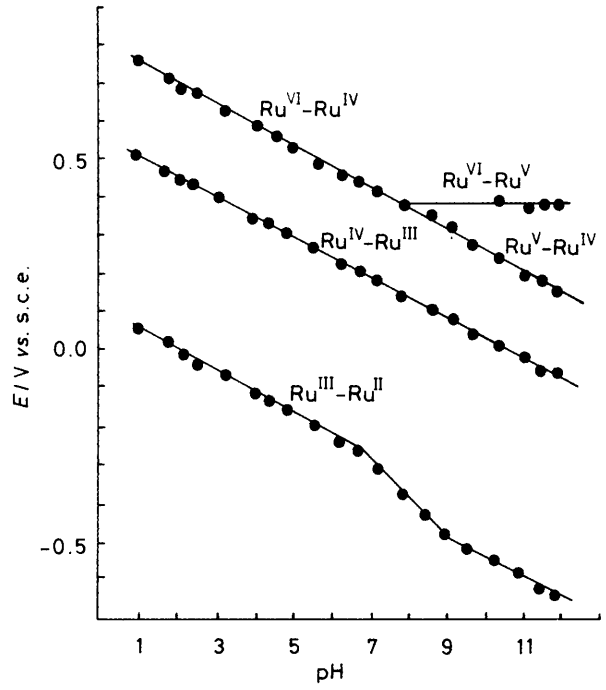

Figure 4. Pourbaix diagram of the formal potentials versus pH of redox couples of *trans*-$[Ru^{VI}L^1(O)_2]^{2+}$

Table 4. The $E°$ values for various redox couples of *trans*-$[Ru^{VI}L^1(O)_2]^{2+}$ at 25 °C

	$E°$/V *vs.* s.c.e.			
			VI–IV	
pH	III–II	IV–III	V–IV	VI–V
1.1	0.07	0.52	0.76	
1.81	0.03	0.48	0.72	
2.21	0.00	0.46	0.70	
2.56	−0.03	0.43	0.68	
3.29	−0.06	0.40	0.64	
4.10	−0.10	0.36	0.60	
4.50	−0.13	0.32	0.57	
5.02	−0.16	0.30	0.54	
5.72	−0.19	0.27	0.51	
6.37	−0.23	0.23	0.47	
6.80	−0.25	0.21	0.45	
7.24	−0.30	0.19	0.42	
7.96	−0.37	0.15	0.40	
8.69	−0.44	0.12	0.36	
9.15	−0.47	0.10	0.35	
9.62	−0.50	0.07	0.29	0.40
10.40	−0.55	0.02	0.26	0.40
11.20	−0.59	−0.02	0.22	0.40
11.58	−0.61	−0.04	0.20	0.40
11.98	−0.63	−0.06	0.18	0.40

For couple I a plot of $E°$ *vs.* pH of the medium over the range pH 1–8 is linear with slope of −60 mV per unit. This is in accordance with a two-electron, two-proton process. At pH 11.58 couple I begins to split into two quasi-reversible one-electron couples IV and V at 0.20 and 0.40 V *vs.* s.c.e. respectively. (Figure 5). Couple V was shown to be independent of pH and couple IV shows a slope of −60 mV/pH. Hence couples IV and V are assigned to the electrode reactions (5) and (6).

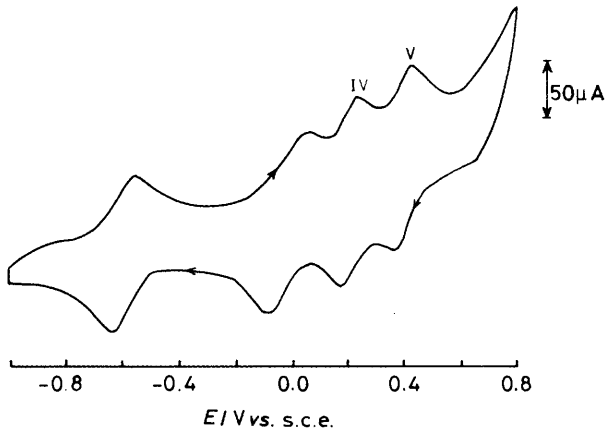

Figure 5. Cyclic voltammogram of *trans*-$[Ru^{VI}L^1(O)_2]^{2+}$ at pH = 11.58, pyrolytic graphite working electrode; scan rate, 50 mV s^{-1}

$$trans\text{-}[Ru^{V}L^1(O)_2]^+ + H^+ + e^- \longrightarrow trans\text{-}[Ru^{IV}L^1(O)(OH)]^+ \quad (5)$$

$$trans\text{-}[Ru^{VI}L^1(O)_2]^{2+} + e^- \longrightarrow trans\text{-}[Ru^{V}L^1(O)_2]^+ \quad (6)$$

The direct reduction of Ru^{VI} to Ru^{IV} in acidic media (pH < 8) is due to the fact that the *trans*-$[Ru^{V}L^1(O)_2]^+$ species undergoes rapid acid catalysed disproportionation in aqueous solution [equation (7)].

$$2\ trans\text{-}[Ru^{V}L^1(O_2)]^+ + 2H^+ \longrightarrow trans\text{-}[Ru^{IV}L^1(O)(H_2O)]^{2+} + trans\text{-}[Ru^{VI}L^1(O)_2)^{2+} \quad (7)$$

Couple II shifts cathodically with a slope of −58 mV/pH corresponding to a one-electron and one-proton process. For couple III, there are three straight-line regions. The slopes are −58, −117, and −58 mV/pH corresponding to the reactions, (3), (8), and (9). From the break points of the plot, the pK_a

$$trans\text{-}[Ru^{III}L^1(OH)(H_2O)]^{2+} + H^+ + e^- \longrightarrow trans\text{-}[Ru^{II}L^1(H_2O)_2]^{2+} \quad (3)$$

pH 1 to 6.8

$$trans\text{-}[Ru^{III}L^1(OH)_2]^+ + 2H^+ + e^- \longrightarrow trans\text{-}[Ru^{II}L^1(H_2O)_2]^{2+} \quad (8)$$

pH 6.8 to 8.9

$$trans\text{-}[Ru^{III}L^1(OH)_2]^+ + H^+ + e^- \longrightarrow trans\text{-}[Ru^{II}L^1(OH)(H_2O)]^+ \quad (9)$$

pH > 8.9

of *trans*-$[Ru^{III}L^1(OH)(H_2O)]^{2+}$ and *trans*-$[Ru^{II}L^1(H_2O)_2]^{2+}$ are 6.9 and 8.9 respectively.

Electrochemistry of trans-$[Ru^{IV}L^1(O)(NCO)]^+$ *in Acetonitrile.*—The cyclic voltammogram of *trans*-$[Ru^{IV}L^1(O)(NCO)]^+$ in acetonitrile at a glassy carbon electrode shows a reversible oxidation couple at 0.96 V *vs.* the ferrocene–ferrocenium couple. The oxidation must be metal centred as the L^1 ligand is electrochemically inactive in this potential range. The peak-to-peak separation and current ratio of this couple are close to 70 mV and unity, respectively at scan rates of 50 to 200 mV s^{-1}, characteristic of a reversible one-electron redox couple. A rotating disc voltammetric study indicated that the magnitude of the limiting current (i_l) is comparable to that for the ferrocene–ferrocenium couple measured under similar con-

Table 5. Stoicheiometric oxidation of organic substrate (100 mg) by *trans*-$[Ru^{VI}L^1(O)_2]ClO_4$ (20 mg) in acetonitrile (2 cm^3) at 25 °C for 5—7 h

Substrate	Product	Yield/%
Isopropyl alcohol	Acetone	100
Benzyl alcohol	Benzaldehyde	100
Cyclohexene	2-Cyclohexene-one	80
	2-Cyclohexenol	20
Toluene	Benzaldehyde	40
Styrene	Benzaldehyde	80
Norborn-2-ene	*exo*-2,3-Epoxynorbornane	30

ditions. Thus the electrode reaction is *trans*-$[Ru^{IV}L^1(O)(NCO)]^+ - e^- \longrightarrow$ *trans*-$[Ru^{V}L^1(O)(NCO)]^{2+}$.

Stoicheiometric Oxidation of Organic Substrates by trans-$[Ru^{VI}L^1(O)_2]^{2+}$.—The oxidation of organic substrates by *trans*-$[Ru^{VI}L^2(O)_2]^{2+}$ was studied previously,[1f] showing it to be a mild oxidant able to oxidize benzyl alcohol to benzaldehyde and isopropyl alcohol to acetone, but failing to react with toluene at room temperature.[1f] For the *trans*-$[Ru^{VI}L^1(O)_2]^{2+}$ complex the redox potential is $\approx$100 mV higher than its L^2 analogue and so would suggest it to be a stronger oxidant. Table 5 summarizes the results of the stoicheiometric oxidative reaction between *trans*-$[Ru^{VI}L^1(O)_2]^{2+}$ and various organic substrates at room temperature. Controlled experiments in the absence of ruthenium complexes were also performed.

It was found that *trans*-$[Ru^{VI}L^1(O)_2]^{2+}$, like the L^2 analogue, can oxidize alcohols to the corresponding aldehydes/ketones. For the oxidation of benzyl alcohol under aerobic conditions, the mole ratio of benzaldehyde to the ruthenium oxidant is greater than one, indicating that *trans*-$[Ru^{VI}L^1(O)_2]^{2+}$ is capable of performing catalytic aerobic oxidation.

The high ν_{asym} (Ru=O) stretching frequency at 860 cm^{-1} for *trans*-$[Ru^{VI}L^1(O)_2]^{2+}$ suggests that this complex has a strong Ru=O bond, which may favour hydrogen atom/hydride abstraction. Thus, with cyclohexene, oxidation occurred at the allylic carbon yielding 2-cyclohexen-1-one as the major product. With styrene, oxidative cleavage of the C=C bond leading to benzaldehyde was the major reaction pathway.

An important difference between *trans*-$[Ru^{VI}L^1(O)_2]^{2+}$ and *trans*-$[Ru^{VI}L^2(O)_2]^{2+}$ is that the former species can oxidize toluene to benzaldehyde. No product resulting from the destruction of the aromatic ring was found, suggesting that attack at the benzylic C–H bond is favoured over oxidation of the aromatic ring. Oxo transfer reaction by *trans*-$[Ru^{VI}L^1(O)_2]^{2+}$ has also been observed, with norborn-2-ene, *exo*-2,3-epoxynorbornane was the sole product of the reaction.

Conclusions

The redox chemistry of the ruthenium oxo complexes of L^1 is very similar to that of their L^2 analogues. Replacement of one tertiary amine by a pyridine functional group in the macrocyclic tertiary amine ligand leads both to an increase in redox potential, and the Ru=O bond length of the *trans*-dioxoruthenium(VI) unit.

Acknowledgements

Financial support from the University of Hong Kong and the Croucher Foundation is gratefully acknowledged. W-O. L. and W-T. W. are Croucher Studentship holders.

References

1 (*a*) C. M. Che, K. Y. Wong, and T. C. W. Mak, *J. Chem. Soc., Chem. Commun.*, 1985, 546; (*b*) *ibid.*, p. 1988; (*c*) C. M. Che, K. Y. Wong, and C. K. Poon, *Inorg. Chem.*, 1985, **24**, 1797; (*d*) C. M. Che and K. Y. Wong, *J. Chem. Soc., Chem. Commun.*, 1986, 22; (*e*) C. M. Che, K. Y. Wong, W. H. Leung, and C. K. Poon, *Inorg. Chem.*, 1986, **25**, 345; (*f*) C. M. Che, T. F. Lai, and K. Y. Wong, *ibid.*, 1987, **22**, 2289; (*g*) C. M. Che and W. H. Leung, *J. Chem. Soc., Chem. Commun.*, 1987, 1376; (*h*) V. W. W. Yam, C. M. Che, and W. T. Tang, *ibid.*, 1988, 100.

2 J. C. Dobson, W. K. Seok, and T. J. Meyer, *Inorg. Chem.*, 1986, **25**, 1514; R. A. Binstead and T. J. Meyer, *J. Am. Chem. Soc.*, 1987, **109**, 3287; J. Gilbert, L. Roecker, and T. J. Meyer, *Inorg. Chem.*, 1987, **26**, 1126; L. Roecker and T. J. Meyer, *J. Am. Chem. Soc.*, 1987, **109**, 746; W. K. Seok, J. C. Dobson, and T. J. Meyer, *Inorg. Chem.*, 1988, **27**, 5; J. C. Dobson and T. J. Meyer, *ibid.*, p. 3283.

3 C. L. Bailey and R. S. Drago, *J. Chem. Soc., Chem. Commun.*, 1987, 179.

4 W. P. Griffith and D. Pawson, *J. Chem. Soc., Dalton Trans.*, 1973, 1316; M. Schroder and W. P. Griffith, *J. Chem. Soc., Chem. Commun.*, 1979, 68; G. Green, W. P. Griffith, D. M. Hollinshead, S. V. Ley, and M. Schroder, *J. Chem. Soc., Perkin Trans. 1*, 1984, 681; W. P. Griffith, S. V. Ley, and A. D. White, *J. Chem. Soc., Chem. Commun.*, 1987, 1625; A. M. El-Hendawy, W. P. Griffith, B. Piggott, and D. J. Williams, *J. Chem. Soc., Dalton Trans.*, 1988, 1983.

5 J. T. Groves and R. Quinn, *Inorg. Chem.*, 1984, **23**, 3844; *J. Am. Chem. Soc.*, 1985, **107**, 5790; J. T. Groves and K-H. Ahn, *Inorg. Chem.*, 1987, **26**, 3831.

6 M. E. Marmion and K. J. Takeuchi, *J. Am. Chem. Soc.*, 1986, **108**, 510; *ibid.*, 1988, **110**, 1472.

7 T. C. Lau and J. K. Kochi, *J. Chem. Soc., Chem. Commun.*, 1987, 179.

8 K. Y. Wong, C. M. Che, and F. C. Anson, *Inorg. Chem.*, 1987, **26**, 737.

9 C. M. Che, S. T. Mak, and T. C. W. Mak, *Inorg. Chem.*, 1986, **25**, 4705.

10 'Enraf-Nonius Structure Determination Package, SDP,' Enraf-Nonius, Delft, 1985.

11 C. M. Che, W. O. Lee, K. W. Fung, and T. C. W. Mak, *J. Chem. Soc., Dalton Trans.*, 1988, 2153.

12 C. K. Poon and C. M. Che, *J. Chem. Soc., Dalton Trans.*, 1980, 756.

13 D. D. Walker and H. Taube, *Inorg. Chem.*, 1981, **20**, 2828.

14 Y. Yukawa, K. Aoyagi, M. Kurihara, K. Shirai, K. Shimizu, M. Mukaida, T. Takeuchi, and H. Kakihana, *Chem. Lett.*, 1985, 283.

Received 5th January 1989; *Paper* 9/00084D